

The Importance of Not Saturating H₂O in Protein NMR. Application to Sensitivity Enhancement and NOE Measurements

Stephan Grzesiek* and Ad Bax*

Laboratory of Chemical Physics
National Institute of Diabetes and
Digestive and Kidney Diseases
National Institutes of Health
Bethesda, Maryland 20892

Received September 17, 1993

It has long been recognized that presaturation of the water resonance is undesirable in many types of protein and nucleic acid NMR experiments, as it obliterates the resonances of rapidly exchanging protons and, via spin diffusion or direct NOE with water, also attenuates the entire ¹H spectrum.¹ A commonly used procedure which avoids the necessity of presaturation uses inhomogeneity of either the radiofrequency field^{2,3} or the static magnetic field^{4,5} to "scramble" the H₂O magnetization during the NMR pulse sequence. Unfortunately, due to the very long T₁ of H₂O protons (4–5 s) compared to protein protons (~1.4 s), the water remains in a semisaturated state as the delay time between scans is typically much shorter than the H₂O T₁. The present Communication describes an approach which, analogous to the original Redfield method,^{1a} leaves the water unperturbed along the B₀ axis during most of the NMR pulse sequence, thereby avoiding ¹H₂O saturation. The approach benefits many of the heteronuclear multidimensional NMR experiments and is demonstrated for ¹H–¹⁵N HSQC correlation,⁶ for quantitative measurement of the ¹⁵N–{¹H} NOE, and for the measurement of NOEs between H₂O and ¹³C-attached protons.^{7,8}

Figure 1A shows the pulse scheme for a nonsaturated ¹H–¹⁵N HSQC correlation. Immediately after the ¹⁵N magnetization is transformed into H₂N_z magnetization (time *a*), the H₂O magnetization is rotated from the *y* to the *-z* axis by the subsequent low-power ¹H 90° pulse. The pulsed field gradient, G₁, ensures that no radiation damping occurs, *i.e.*, the H₂O magnetization remains along *-z* until, *t*₁/2 later, the ¹H 180° pulse returns it to *+z*. The final ¹H 90° pulse (time *b*) is preceded by a shaped 90° pulse on H₂O, and, similarly, the final ¹H 180° pulse is surrounded by low-power 90° pulses and by pulsed field gradients (G₃).⁹ This leaves the H₂O magnetization in a well-defined state along the *z* axis, providing excellent water suppression.

Results are shown for the backbone amides of Leu⁶⁹–Arg⁹⁰ in a 1.2 mM sample of [¹⁵N]calmodulin (CaM) complexed with a peptide fragment, known as M13, of skeletal muscle myosin light chain kinase. Figure 2A shows the decrease in ¹H–¹⁵N HSQC correlation intensity observed using H₂O presaturation (filled circles) or a scrambling pulse³ (open circles) relative to the water flip-back HSQC experiment of Figure 1A. In the NMR structure of the CaM/M13 complex,¹⁰ residues 67–73 and 83–92 are in an α -helical arrangement, whereas Arg⁷⁴–Glu⁸² form a solvent-

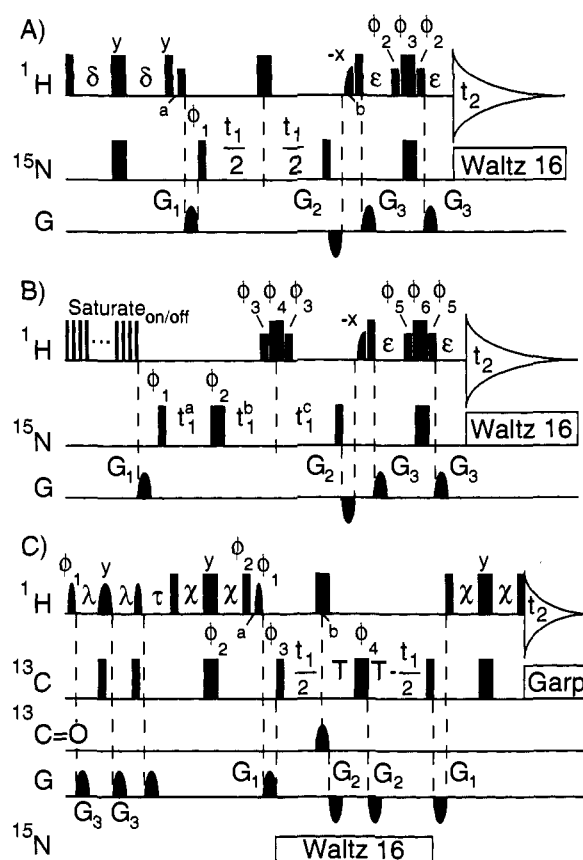


Figure 1. Pulse sequence for water flip-back versions of (A) ¹H–¹⁵N HSQC, (B) ¹⁵N–{¹H} NOE, and (C) water–NOE difference constant-time ¹H–¹³C HSQC experiments. Narrow and wide pulses denote 90° and 180° flip angles, respectively. Unless indicated, pulses are applied along the *x* axis. Low-intensity rectangular pulses are applied with a radiofrequency field strength of ~250 Hz. Half-Gauss (schemes A and B) and sine bell (C)-shaped 90° pulses are 2.1 ms (4.2 ms for 180° in C). Pulsed field gradients are sine bell-shaped (25 G/cm at center); G_{1,2,3} = 2.5, 1.0, 0.4 ms. Delays: δ = 2.25 ms; ϵ = 1.25 ms; λ = 2.4 ms; χ = 1.5 ms; 2*T* = 27 ms; τ = 100 ms (NOE mixing). For (B), *t*₁^a = (1 – *t*₁/*t*_{1max}) × 2.5 ms; *t*₁^b = *t*₁/2 – (*t*₁/*t*_{1max}) × 2.5 ms; *t*₁^c = *t*₁/2 + 2.5 ms. Phase cycling: (A) $\phi_1 = x, -x$; $\phi_2 = -\phi_3 = x, x, -x, -x$; Rec. = *x, -x*. (B) $\phi_1 = y, -y$; $\phi_2 = 4(x), 4(y), 4(-x), 4(-y)$; $\phi_3 = \phi_4 = 16(x), 16(-x)$; $\phi_5 = -\phi_6 = x, x, -x, -x$; Rec. = *x, -x, x, -x, x, -x, x, -x*. (C) $\phi_2 = y, -y$; $\phi_3 = x, x, -x, -x$; Rec. = *x, -x, -x, x*. For C, transients with $\phi_1 = x$ and $\phi_1 = -x$, are recorded in an interleaved manner and stored separately.

exposed flexible loop. As expected, the increase in signal-to-noise (S/N) is greatest for protons in the loop region, for which previously high hydrogen exchange rates were reported.¹¹ However, an appreciable increase in sensitivity (10–20%) is also observed for slowly exchanging amide protons and for carbon-attached protons (data not shown).

A second example of avoiding saturation of the H₂O signal concerns the measurement of heteronuclear ¹⁵N–{¹H} NOE values, important for quantitating the degree of internal protein dynamics.^{12–14} These NOE values are measured by comparing the intensity of signal transferred from ¹⁵N to ¹H^N in the absence and presence of ¹H saturation. Magnetization exchange between amide protons and water protons, either via (exchange-mediated) NOE or hydrogen exchange, can cause amide protons to relax to their thermal equilibrium value with a time constant that can

(1) (a) Redfield, A. G.; Kunz, S. D.; Ralph, E. K. *J. Magn. Reson.* **1975**, *19*, 114–117. (b) Guéron, M.; Plateau, P.; Decors, M. *Prog. NMR Spectrosc.* **1991**, *23*, 135–209.

(2) Sklenar, V.; Bax, A. *J. Magn. Reson.* **1987**, *75*, 378–383.

(3) Messerle, B. A.; Wider, G.; Otting, G.; Weber, C.; Wüthrich, K. *J. Magn. Reson.* **1989**, *85*, 608–613.

(4) John, B. K.; Plant, D.; Heald, S. L.; Hurd, R. E. *J. Magn. Reson.* **1991**, *94*, 664–669.

(5) Kay, L. E.; Keifer, P.; Saarinen, T. *J. Am. Chem. Soc.* **1992**, *114*, 10663–10665.

(6) Bodenhausen, G.; Ruben, D. *J. Chem. Phys. Lett.* **1980**, *69*, 185–188.

(7) Otting, G.; Liepinsh, E.; Wüthrich, K. *Science* **1991**, *254*, 974–980.

(8) Qian, Y. Q.; Otting, G.; Wüthrich, K. *J. Am. Chem. Soc.* **1993**, *115*, 1189–1190.

(9) Piotto, M.; Saudek, V.; Sklenar, V. *J. Biomol. NMR* **1992**, *2*, 661–665.

(10) Ikura, M.; Clore, G. M.; Gronenborn, A. M.; Zhu, G.; Klee, C. B.; Bax, A. *Science* **1992**, *256*, 632–638.

(11) Spera, S.; Ikura, M.; Bax, A. *J. Biomol. NMR* **1991**, *1*, 155–165.

(12) Kay, L. E.; Torchia, D. A.; Bax, A. *Biochemistry* **1989**, *28*, 8972–8979.

(13) Clore, G. M.; Driscoll, P. C.; Wingfield, P. T.; Gronenborn, A. M. *Biochemistry* **1990**, *29*, 7387–7401.

(14) Stone, M. J.; Fairbrother, W.; Palmer, A. G.; Reitzer, J.; Sayer, M. H.; Wright, P. E. *Biochemistry* **1992**, *31*, 4394–4406.

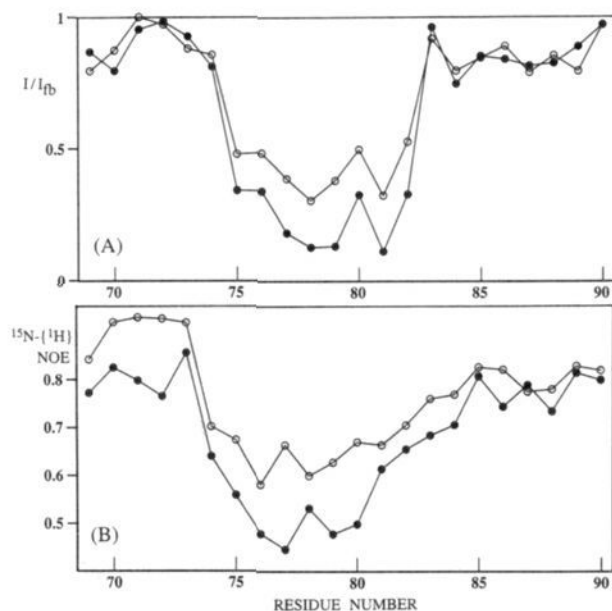


Figure 2. (A) Intensity, I , of HSQC $^1\text{H}\text{-}^{15}\text{N}$ correlations for residues 69–90 in $[\text{U}\text{-}^{15}\text{N}]\text{CaM}\text{-M13}$, recorded with H_2O presaturation ($\gamma B_1/2\pi = 20$ Hz) (●) or a scrambling pulse³ (1 ms) (○) versus the intensity (I_{fb}) obtained with a water flip-back HSQC (Figure 1A). (B) $^{15}\text{N}\{-^1\text{H}\}$ heteronuclear NOE values measured without (○) and with water flip-back (●), using the scheme of Figure 1B. Both sets of measured NOE values (NOE_m) have been corrected for incomplete ^1H T_1 recovery by $\text{NOE} = [1 - \exp(-T/T_1)]\text{NOE}_m/[1 - \exp(-T/T_1)\text{NOE}_m]$, where T is the recovery delay (3.1 s) and T_1 is the protein ^1H T_1 (1.4 s). The root mean square error in the NOE values is ~ 0.04 . Spectra are recorded at 35 °C, 600 MHz, pH 6.6.

be much longer than their inherent T_1 . For reasons of sensitivity, the experiment is frequently repeated with a delay between scans of only $\sim 3\text{--}4$ s,^{12–14} shorter than the T_1 of the H_2O resonance. As a consequence, unless special precaution (Figure 1B) is taken to avoid saturation of H_2O , the reference signal (with no NOE) for an amide subject to hydrogen exchange may be much smaller than its true equilibrium value. Figure 2B compares the $^{15}\text{N}\{-^1\text{H}\}$ NOE values for Leu⁶⁹–Arg⁹⁰ in CaM/M13 measured with the original pulse scheme¹² with values obtained with the scheme of Figure 1B. Clearly, significantly lower NOE values, indicating more disorder, are measured if care is taken to avoid saturation of H_2O . The lowest values for the $^{15}\text{N}\{-^1\text{H}\}$ NOE are found for Lys⁷⁵–Thr⁸⁰, near the center of the previously defined¹⁰ solvent-exposed loop. In the X-ray structure of a complex between CaM and a peptide fragment of smooth muscle myosin light chain kinase (30% homology with M13), this loop extended from Ala⁷³ to Lys⁷⁷.¹⁵ The present data indicate that the shift in loop position between the NMR and crystal structures of the two peptide/CaM complexes is not caused by the fact that the NMR structure was calculated from only ~ 1800 NOEs.

As a final example, we illustrate the importance of not saturating the H_2O resonance for measurement of NOE interactions between aliphatic protons and water. Figure 1C shows the pulse scheme used, which is essentially a simple 2D version of the 3D ^{13}C -separated NOESY experiment.⁸ The first low-power ^1H $90^\circ_{\phi_1-\lambda-180^\circ_{\phi_2}-90^\circ_x$ pulses serve to invert ($\phi_1 = x$) or not invert ($\phi_1 = -x$) the H_2O resonance, whereas the first two 90° ^{13}C purge pulses ensure that magnetization from H^α protons resonating under the H_2O line are eliminated. During the following NOE mixing period, τ , only magnetization from water protons is then transferred to the protein, and its protons are subsequently dispersed in the ^{13}C dimension by a constant-time

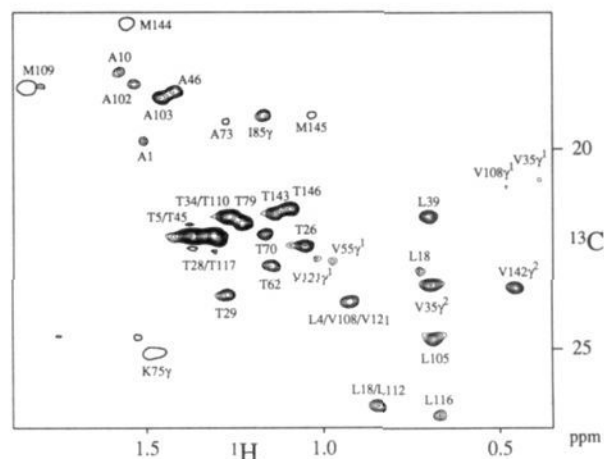


Figure 3. Methyl region of the $^1\text{H}\text{-}^{13}\text{C}$ CT-HSQC difference spectrum, displaying NOE interactions with water in the $[\text{U}\text{-}^{13}\text{C}, ^{15}\text{N}]\text{CaM}\text{-M13}$ complex (1.5 mM), recorded at 27 °C, 100 ms NOE mixing time, 600 MHz, pH 6.6. Total recording time, 13.5 h. The CT-HSQC spectrum has been recorded with $2T = 1/J_{CC} = 27$ ms, and correlations for carbons coupled to odd and even numbers of aliphatic carbons are of opposite sign.¹⁶ Single bold contours denote negative resonances.

HSQC scheme.¹⁶ After the creation of H_2C_z magnetization by the first INEPT (time a), a selective 90° pulse returns the water to the positive z axis. The 180° ^1H pulse (time b) which serves to decouple ^{13}C from ^1H takes the H_2O magnetization to $-z$, and the first G_2 gradient ensures that no radiation damping takes place after this pulse. The final $90_x\text{-}\chi\text{-}180_y\text{-}\chi\text{-}90_x$ ^1H pulses are part of the last reverse INEPT transfer but also return the water magnetization from $-z$ to $+z$. Hence, the water is flipped back to $+z$ at the end of every scan, eliminating saturation and thereby maximizing NOE transfer from H_2O to protein.

Figure 3 shows the methyl region of the water flip-back HSQC NOE spectrum, applied to the CaM/M13 complex. A substantial number of resonances in this region show strong cross peaks, indicative of NOE to water. Except for the weak cross peak of Ala⁷³– $\text{C}\gamma\text{H}_3$, the signs of all cross peaks are indicative of negative NOEs. Resonances seen for Lys– $\text{C}\gamma$ and Thr– $\text{C}\gamma$ very likely reflect intraresidue NOEs to the rapidly exchanging side-chain amino and hydroxyl protons, which are indistinguishable from direct NOEs to water.⁸ To investigate the possible presence of tightly bound water in the calmodulin–peptide complex, analysis of the NOEs observed to other methyl groups and to many other side-chain protons outside the region shown in Figure 3 is presently in progress.

The large molar excess of slowly relaxing water protons provides a precious reservoir of nuclear spin magnetization. It can be used either to measure NOE interactions between water and protein or to rapidly restore to thermal equilibrium the magnetization of exchangeable protons, which usually yield the weakest NMR signals. This can enhance the sensitivity in many different types of 2D and 3D experiments. In other cases, such as the study of heteronuclear $^{15}\text{N}\{-^1\text{H}\}$ NOE or water–protein NOE interactions, the water flip-back procedure can eliminate substantial errors in quantitative measurement.

Acknowledgment. We thank Dennis Torchia and Andy Wang for useful comments and Rolf Tschudin for technical support. This work was supported by the Intramural AIDS Targeted Anti-Viral Program of the Office of the Director of the National Institutes of Health.

(15) Meador, W. E.; Means, A. R.; Quijoco, F. A. *Science* **1992**, *257*, 1251–1255.

(16) Vuister, G. W.; Bax, A. *J. Magn. Reson.* **1992**, *98*, 428–435.